Photodiagnosis and Photodynamic Therapy 28 (2019) 88–97

Contents lists available at ScienceDirect

Photodiagnosis and Photodynamic Therapy

journal homepage: www.elsevier.com/locate/pdpdt

Photodynamic therapy using zinc phthalocyanine with low dose of diode laser combined with doxorubicin is a synergistic combination therapy for human SK-MEL-3 melanoma cells

Mohammad Amin Doustvandi[a], Fateme Mohammadnejad[a], Behzad Mansoori[a,b,e], Habib Tajalli[c,d], Ali Mohammadi[a,e], Ahad Mokhtarzadeh[a,f], Elham Baghbani[a,b], Vahid Khaze[a], Khalil Hajiasgharzadeh[a], Mahsa Maleki Moghaddam[a], Michael R. Hamblin[g], Behzad Baradaran[a,*]

[a] Immunology Research Center, Tabriz University of Medical Sciences, Tabriz, Iran
[b] Student Research Committee, Tabriz University of Medical Sciences, Tabriz, Iran
[c] Research Institute for Applied Physics and Astronomy, University of Tabriz, Tabriz, Iran
[d] Biophotonic Research Center, Islamic Azad University, Tabriz Branch, Tabriz, Iran
[e] Department of Cancer and Inflammation Research, Institute of Molecular Medicine, University of Southern Denmark, Odense, Denmark
[f] Department of Biotechnology, Higher Education Institute of Rab-Rashid, Tabriz, Iran
[g] Wellman Center for Photomedicine, Massachusetts General Hospital, Boston, MA, USA

ARTICLE INFO

Keywords:
PDT
Diode laser
Zinc phthalocyanine
Doxorubicin
Combination therapy
Synergism
SK-MEL-3 cell line
Melanoma

ABSTRACT

Chemotherapy is a generally used anticancer strategy for melanoma and it may have improved outcomes in combination with other approaches. One such strategy is photodynamic therapy (PDT), where a photosensitizer (PS) generates reactive oxygen species (ROS) after illumination of target cells. Interestingly, in low doses and high doses of light sources, special cellular responses can be induced. Regarding this fact, in this study, the combination of zinc phthalocyanine (ZnPc)-PDT and Doxorubicin (DOX) was applied at low and high dose of diode laser to treat SK-MEL-3 cells. Cytotoxic effects were determined by MTT assay for assessment synergistic effects were estimated by calculation of Combination Index (CI); that synergistic effects were observed in most groups. In low dose of laser irradiation higher synergism effects were observed. Significant changes of ROS were not observed with combinations, but autophagy, subG1 and G2/M phase cell cycle arrest, decreased cell migration ability and apoptosis induction were significantly increased compared to either treatment alone. The expression of caspase-8, -9, -3 and Bcl-2 genes revealed caspase-dependent apoptosis in all groups. Moreover, ZnPc-PDT and chemo-PDT down-regulated the expression of MMP-9 and Vimentin genes that impaired cell migration. In conclusion, it can be suggested that pre-treatment with ZnPc-PDT has high effects to sensitize SK-MEL-3 cells to DOX, in particular with low dose of diode laser.

1. Introduction

Malignant Melanoma is the most common aggressive skin cancer worldwide. As reported by the American Cancer Society, about 91,270 new cases of melanoma were approximated to be detected in 2018. About 9,320 Americans are estimated to die from melanoma in 2018 [1]. Heavy prices are spent every year on research in order to treat melanoma or improve the quality of life in patients. The most common strategies of melanoma treatment are surgery, radiation therapy and chemotherapy [2]. Chemotherapy is a commonly used anticancer approach and has been significantly developed to date [3]. Nevertheless, serious side effects and drug-resistance can lead to limited therapeutic outcomes of chemotherapy in most kinds of cancers such as melanoma [4–6]. Owing to the heterogeneity and rapid proliferation of melanoma cells along with the high probability of melanoma invasion and metastasis [5], any single treatment approach is generally not sufficient to

* Corresponding author at: Immunology Research Center, Tabriz University of Medical Sciences, Tabriz, 5166614766, Iran.
E-mail addresses: m.amin.dostvandi@gmail.com (M.A. Doustvandi), fatememohamadnejad@gmail.com (F. Mohammadnejad), bmansoori@health.sdu.dk (B. Mansoori), habibtajalli@yahoo.com (H. Tajalli), bmansoori@health.sdu.dk (A. Mohammadi), ahad.mokhtarzadeh@gmail.com (A. Mokhtarzadeh), E_baghban49@yahoo.com (E. Baghbani), V_khazee@yahoo.com (V. Khaze), hajiasgharzadeh@yahoo.com (K. Hajiasgharzadeh), mahsa.maleki225@gmail.com (M.M. Moghaddam), hamblin@helix.mgh.harvard.edu (M.R. Hamblin), behzad_im@yahoo.com (B. Baradaran).

https://doi.org/10.1016/j.pdpdt.2019.08.027
Received 1 June 2019; Received in revised form 1 August 2019; Accepted 23 August 2019
Available online 24 August 2019
1572-1000/

destroy the entire tumor [7]. Combination therapy using two or more therapeutic agents either simultaneously or sequentially has been explored since the 1960s, in order to improve the effectiveness of cancer therapy [8–10]. Combination therapy shows better therapeutic results when compared to single therapies, especially in reducing drug-resistance and preventing cancer recurrence. Combination therapy can also decrease side effects and improve the survival rate in cancer patients [7].

The combination of chemotherapy with photodynamic therapy (PDT) has received significant attention as a promising approach to treat cancer [11–13]. PDT is an effective minimally-invasive approach to the treatment of cancers of different types and sites as well as non-cancerous diseases. Excellent therapeutic results and capability of the parallel application of PDT with other treatments make it attractive [14]. PDT is based on local or systemic administration of a photoactive agent (photosensitizer), which is selectively accumulated in the tumor. The photosensitizer molecules absorb light of the specific wavelength and produce reactive oxygen species (ROS) inducing a biological cascade leading to selective death of the targeted cells. In the treatment of melanoma with PDT immediately suggests the question of the interaction of light with endogenous molecules of skin (such as melanin and hemoglobin) which absorb light. The most appropriate wavelength for PDT is 600–800 nm, which is known as the “therapeutic window”. Melanin and hemoglobin exhibit absorption across the visible region of the spectrum, but both fall to a minimum level in the therapeutic window [15,16].

Research over the last decades has shown that the use of two or more therapeutic approach in cancer treatment has more effective results than the single therapy approach. Notwithstanding the success of combined chemotherapy with DOX and ZnPc-PDT (chemo-PDT,) identify the most important factors and innovative methods are yet being researched and needed to improve the effective use of chemo-PDT in clinical oncology. Although PDT and chemotherapy have shown high potential for cancer therapy, both strategies have complex limitations, such as high side effects and drug-resistance (for chemotherapy) and difficulty in the light delivery of some internal tumors (for PDT). Biological mechanisms and effective factors of chemo-PDT effectiveness are extremely intricate and not completely identified to date. In this regard, the purpose of this work are (I) the comparative study of effects of low and high dose of light source in combination ZnPc-PDT with DOX to investigate the role of light source in chemo-PDT synergistic outcomes; (II) the comparative study of cellular and molecular mechanisms after chemo-PDT to highlighting significant results. So, we characterizing these mechanisms aimed at maximizing therapeutic outcomes with minimum invasive effects by employing the advantages of both strategies.

2. Materials and methods

2.1. Cell line and cell culture

Human melanoma cell line (SK-MEL-3) was obtained from the Pasteur Institute of Iran. The cells were cultured in Roswell Park Memorial Institute (RPMI) 1640 medium supplemented with 10% fetal bovine serum (Gibco, USA) and 1% antibiotics (penicillin /streptomycin, Gibco, USA). Subsequently, cells were incubated in the incubator at 37 ˚C under an atmosphere of 5% CO2 and 95% humidity.

2.2. In vitro cellular uptake of ZnPc

According to our previously reported article [17], DMSO was used to make ZnPc dissolve in the culture medium. The total concentration of DMSO in the stock solution (18 μM) was reached 2% (v/v) in RPMI1640. In this sense, ZnPc was firstly dissolved in DMSO and RPMI1640 by sonication, and then all the concentrations (0.00002–9 μM) tried in the experiments were diluted using RPMI1640. The cellular uptake of ZnPc was determined by fluorescence intensity measurement by using flow cytometry (MacsQuant10 Analyser, Miltenyi Biotech, Germany). After reaching almost 75% confluency of cells, they were seeded in 6-well-plate and was kept for 24 h in the incubator. The culture medium with different concentrations (0.00002–9 μM) of ZnPc was added to each group. Subsequently, the cells were further incubated for 24 h in the incubator, respectively followed by washed thrice with PBS (Phosphate Buffered Saline), trypsinized and centrifuged at 1300 rpm for 8 min, and suspended with PBS.

2.3. Cytotoxicity effects of PDT with ZnPc and chemotherapy with DOX

For invitro treatment with PDT, firstly, the cells were seeded in 96-well plates and were kept for 24 h in the incubator. Then, the cells were treated with different concentrations of ZnPc (0.00002–9 μM) for overnight. Next, the cells were washed thrice with PBS and added fresh culture medium to wells. Finally, the cells were exposed by 675-nm light using a diode laser at low and high dose of laser (5 J/cm^2 with duration of irradiation ~ 12(s) and 20 J/cm^2 with duration of irradiation ~ 50(s)) in the dark room. Similarly, to determine the DOX cytotoxicity, the cells were treated with DOX at different concentrations (0.00002–9 μM) for 24 h. For MTT assays, 24 h after laser irradiation and DOX treatment, 50 μl (2 mg/ml) of MTT solution (methylthiazole tetrazolium, Sigma Aldrich, USA) was added to all groups and incubated at 37 °C for 4 h. Next, 200 μl DMSO was added to all wells and incubated for 30 min at 37 °C.

Optical density (OD) of all wells was assessed by an ELISA reader (Sunrise ELISA Plate Reader, Tecan, Salzberg, Austria).

2.4. PDT in combination with DOX (chemo- PDT)

To determine probable synergetic effects of cytotoxicity of PDT and DOX, firstly, the cells were treated with two doses of ZnPc-PDT (IC25 and IC50) and immediately afterward the cells were incubated with DOX (0.00002–9 μM) for overnight. The MTT assays were performed 24 h after incubation with DOX.

2.5. Measurement of reactive oxygen species

To assess reactive oxygen species (ROS), the cells were classified into different groups. The first group, defined as the control group, received neither PDT nor DOX. The second group was treated with PDT without DOX, the third group, was treated only with DOX without PDT. The final group, defined as chemo-PDT, was treated with both PDT and DOX. Then, cells were treated with DCFH-DA (100 μM, Sigma Aldrich, USA) at the incubator for 40 min. After the cells were washed thrice with PBS, the generation of ROS was measured using a flow cytometer (MacsQuant Analyser 10, Miltenyi Biotech, Germany).

2.6. Detection of autophagic cells with monodansyl cadaverine (MDC) staining

To perform all experiments in this work, cells were categorized similar to that in the ROS assays. Therefore, the MDC (Sigma Aldrich, USA) staining was performed for the measurement of autophagic cells after treatments. Briefly, 24 h after treatments, the cells were washed with PBS and incubated with MDC at concentration of 50 μM for 10 min at 37∘C. After incubation, the cells were washed thrice with PBS and evaluation of autophagic cells was investigated using a live cells imaging system (Citation 5, Biotek, CA) and a flow cytometer (MacsQuant Analyser 10, Miltenyi Biotech, Germany).

2.7. Detection of acidic organelles

Acidic organelles were monitored by using LysoTracker Red DND-

99 (Invitrogen, USA). For this, after described treatments, cells were incubated with 50 nM Lysotracker Red DND-99 in culture medium for 35 min at 37 °C. After 35 min, the LysoTracker Red was removed and washed thrice with PBS. Finally, acidic organelles were observed immediately by using a live cells imaging system (Citation 5, Biotek, CA).

2.8. Detection of apoptotic cells

2.8.1. Annexin V/PI assay

The rate of apoptosis after desired treatments was assessed by flow cytometry (MacsQuant Analyser10, Miltenyi Biotech, Germany) using ApoFlowEx® FITC Kit (EXBIO, Czech Republic). 24 h after treatments, the SK-MEL-3 cells were trypsinzed and centrifuged at 1300 rpm for 8 min. The cells were suspended in binding buffer, then added 5 µl of Annexin-V- FITC and kept for 15 min at room temperature in the dark. Afterward, the cells were again centrifuged at 1300 rpm for 8 min and resuspended in binding buffer and were added 5 µl of PI. Finally, percentages of apoptotic cells were determined by using flow cytometry.

2.8.2. DAPI staining

The fragmentation of the nucleus was also observed by the live cells imaging system (Citation 5, Biotek, CA). The cells were treated as described above, then, the cells were fixed with 4% paraformaldehyde for 20 min. After thrice washes with PBS, cells were penetrable by 0.01% Triton-X-100 for 15 min. After another thrice washes with PBS, cells were stained with DAPI nuclear stain solution for 10 min in the dark room and observed under live cells imaging system.

2.9. Quantitative real-time PCR analysis

Following the mentioned treatments, quantitative real-time PCR (qRT-PCR) was performed. Total RNA was extracted with the use of the GeneAll RiboEx LS RNA extraction kit (GeneAll Biotech, Korea). Then, mRNAs were reverse transcribed toward cDNA with cDNA Synthesis Kit (BioFact, Korea), using the manufacturer's protocols. qRT-PCR tests were performed by using a standard SYBR Green PCR master mix (Ampliqon, Denmark) protocol in the Roche Light Cycler 96 system. GAPDH was used as a reference for caspase -8, -9, -3, Bcl2, MMP-9 and Vimentin. The relative expression levels of genes were normalized with an internal control (GAPDH) by using $2^{-\Delta\Delta Ct}$ cycle threshold method. Sequences of primers are shown in Table 1.

2.10. Cell cycle assay

The cell cycle distribution was analyzed after treatments with flow cytometry (MacsQuant Analyser10, Miltenyi Biotech, Germany). The cells were washed thrice with PBS and fixed by 75% (v/v) ethanol at 4 °C for overnight. Then, fixed cells were centrifuged for removal of ethanol and suspended in PBS containing RNase A (Carl Roth, Karlsruhe, Germany) at 37 °C for 30 min. Next, the cells were again centrifuged and the PI staining solution (0.01% Triton X-100, 0.01% PI) was added for 10 min in the dark-room and the cell cycle distribution was analyzed.

Table 1
Primers sequences.

Genes	Primer sequences
Bcl-2	Forward: 5′ CCTGTGGATGACTGAGTACC 3′ Reverse: 5′ GAGACAGCCAGGAGAAATCA 3′
Caspase-8	Forward: 5′ GGTCTGAAGGCTGGTTGTTC 3′ Reverse: 5′ AATCTCAATATTCCCAAGGTTCAAG 3′
Caspase-9	Forward: 5′ CCGGAATCCTGCTTGGGTATC 3′ Reverse: 5′ CATCGGTGCATTTGGCATGTA 3′
Caspase-3	Forward: 5′ TGTCATCTCGCTCTGGTACG 3′ Reverse: 5′ AAATGACCCCTTCATCACCA 3′
Vimentin	Forward: 5′ GCGCACAAATCCCTTCTACC 3′ Reverse: 5′ ATCCGTGTAGCACATTCTGTCC 3′
MMP-9	Forward: 5′ GGTTCTTCTGCGCTACTGCTG 3′ Reverse: 5′ GTCGTAGGGCTGCTGGAAGG 3′
GAPDH	Forward: 5′ CCTCGTCCCGTAGACAAAA 3′ Reverse: 5′ AATCTCCACTTTGCCACTG 3′

2.11. Wound healing assay

To investigate the migration and invasion capability of SK-MEL-3 cells, after carrying out the above-mentioned treatments, the cells were scratched by sterile yellow pipette tips across the cell monolayer to form an artificial wound gap. At different times after treatment (from 0 h to 24 h) the cells on the plate were photographed under the inverted microscope (Optika, Italy) and the migration ability of SK-MEL-3 cells was determined.

2.12. Statistical analysis

Data were presented as means ± standard deviation (SD) of at least three independent experiments. Significant differences were detected by one-way and/or two-way ANOVA followed by Dunnett's multiple comparisons test implemented by GraphPad Prism 6 statistical (Software, La Jolla, CA, USA). A p value < 0.05 was considered statistically significant.

The interactions between ZnPc-PDT and DOX were evaluated with the Chou-Talalay method. For, x% toxicity, the combination index (CI) values were calculated based on the equation stated below:

$$CI = (D)_1 / (D_X)_1 + (D)_2 / (D_X)_2 + (D)_1.(D)_2 / (D_X)_1 (D_X)_2$$

3. Results and discussion

The role of the light source used in PDT is highly complex and remarkable. So, characterizing roles of the light source in synergistic effects of combination therapy leads to design better PDT and chemo-PDT protocols that extensively improve these efficiencies. Although the use of chemotherapy and PDT are clinically extended, the mechanisms underlying cancer cells death after chemo-PDT and effective factors are not completely characterized. In fact, one of the main areas of studies in the cancer treatment has been reported of cellular and molecular pathways after treatment, in relation to migration and invasion ability, cell cycle regulation, genes expression, autophagy, apoptosis and necrosis. Some of these pathways are activated by PDT, chemotherapy and as well as chemo-PDT [18–20]. Researches and an understanding of the role of effective factors in PDT, chemotherapy and chemo-PDT on cellular and molecular pathways, may to result in the optimization of chemo-PDT as a cancer treatment modality.

3.1. Invitro cellular uptake of ZnPc

The efficacy of PDT, to a great extent, depends on cellular uptake and intracellular accumulation of photosensitizer [21–23]. ZnPc tends to self-aggregation in biological media and aggregation decreases the photosensitizing capability and uptake of ZnPc. The aggregation of the ZnPc could be reduced in such solvents as DMF and DMSO (dimethylsulfoxide) [24]. It is noteworthy mentioning that ZnPc has a strong absorption peak at 675 nm and the intensity of fluorescence has a positive correlation with the uptake of ZnPc [25]. So, to enquire whether ZnPc was uptaken by cells, flow cytometry was used in the try out. The SK-MEL-3 cells were treated with different concentration of ZnPc without laser irradiation. After 24 h, the intensity of ZnPc fluorescence was measured and shown in Fig. 1. We found that ZnPc was extensively taken up with cells and it was in of concentration-dependent manner.

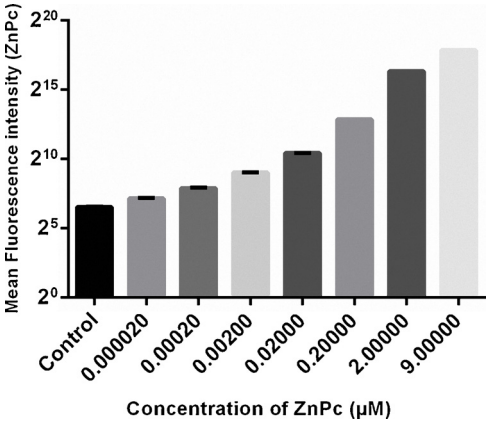

Fig. 1. Invitro cellular uptake of ZnPc. The cells were incubated with 0, 0.00002, 0.0002, 0.002, 0.02, 0.2, 2 and 9 μM of ZnPc for 24 h and fluorescence intensity showed extensive cellular uptake of ZnPc in concentration-dependent manner.

3.2. Cytotoxicity effects of ZnPc-PDT and DOX alone

Based on the cellular uptake of ZnPc studies, the PDT with ZnPc and chemotherapy with DOX were evaluated. The MTT results (Fig. 2) of cytotoxicity assessment of DOX and ZnPc-PDT after 24 h incubation, led to induction of concentration-dependent cell death.

The IC50 and IC25 values of ZnPc in low and high dose of laser (5 and 20 J/cm^2) were 0.145 ± 0.01, 0.062 ± 0.01 and 0.012 ± 0.01, 0.007 ± 0.01 μM (Table 2), respectively. Also, the IC50 value of DOX after 24 h was 7.764 ± 0.01 μM (Table 2). In addition, the MTT results showed that light source without ZnPc and ZnPc without light source had no palpable phototoxic and cytotoxic effects on cells. The obtained data were indicating the high phototoxic effects of ZnPc and cytotoxic effects of DOX at low concentrations.

Table 2
IC50 and IC25 values of DOX, ZnPc-PDT and chemo-PDT against SK-MEL-3 cells.

Sample	IC_{50} values (μM)		IC_{25} values (μM)	
	ZnPc (μM)	DOX (μM)	ZnPc (μM)	DOX (μM)
DOX	_	7.764 ± 0.01	_	_
ZnPc-PDT,5 J/cm^2	0.145 ± 0.01	_	0.012 ± 0.01	_
ZnPc-PDT, 20 J/cm^2	0.062 ± 0.01	_	0.007 ± 0.01	_
Chemo-PDT, 5 J/cm^2	0.012 ± 0.01	0.0005 ± 0.01	_	_
Chemo-PDT, 20 J/cm^2	0.007 ± 0.01	0.0018 ± 0.01	_	_

3.3. Cytotoxicity and synergism effects of chemo- PDT using ZnPc and DOX

In this study, the IC50 and IC25 values of ZnPc-PDT have then selected for the determination Combination Index (CI) studies. The CI was calculated using the Chou-Talalay method. The estimation of CI values allows a quantitative definition for antagonism (CI > 1.0); additive effects (CI = 1.0) and synergism (CI < 1.0) [26]. Cytotoxic effects of chemo-PDT were determinate by the MTT test and set as the IC50 values of chemo-PDT on SK-MEL-3 cells (Fig. 2C). Synergistic outcomes after the combination of ZnPc-PDT in low and high dose of laser (5, 20 J/cm^2) with DOX were observed in combination groups (CI < 1.0) (Fig. 2D). But, in the low dose of laser (5 J/cm^2) higher synergism effects were observed; thus, in this dose of chemo-PDT, the synergism effects were more promising in SK-MEL-3 cells. In fact, pre-treatment with ZnPc-PDT at low dose of laser can lead to more reduced the dose of DOX used in chemotherapy and increased the sensitivity of SK-MEL-3 cells to the very low concentrations of the DOX. Accordingly, we can reduce the serious side effects of DOX, which has a positive correlation with its concentration, and significantly reduced the resistance of melanoma cells to this chemo-drug.

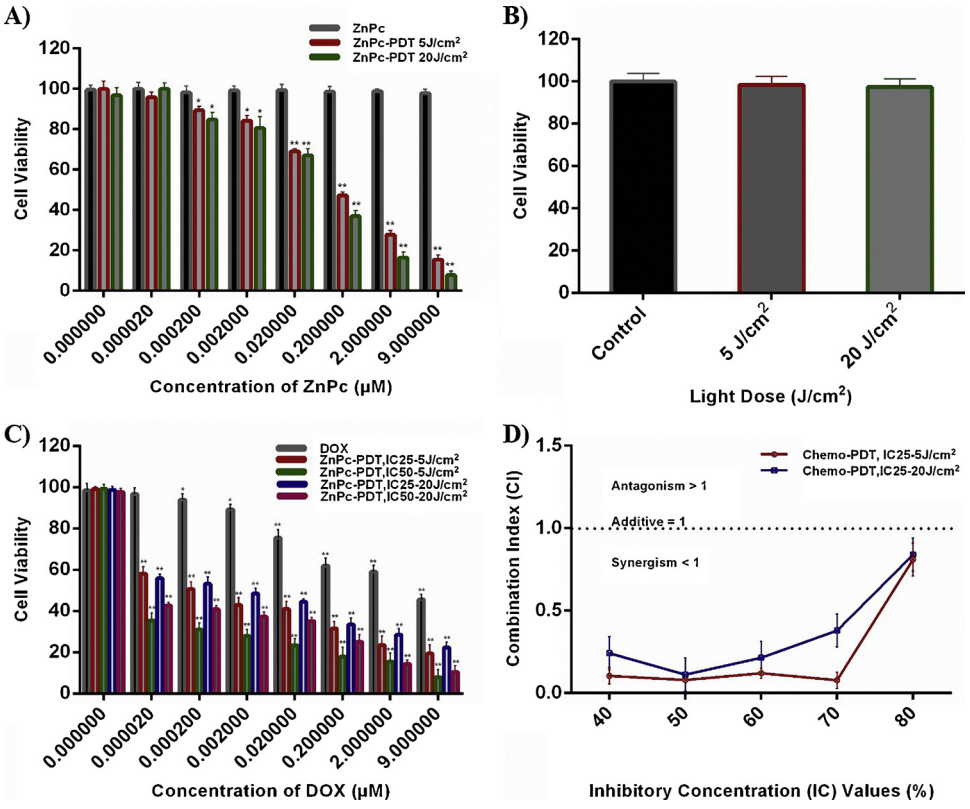

Fig. 2. The cytotoxic effects of ZnPc-PDT, light source, DOX, chemo-PDT and Combination Index: (A) Cell viability in presence of different concentrations of ZnPc (with or without light sources); (B) The effects of light sources (without ZnPc) with 5 and 20 J/cm^2 fluence; (C) Cell viability in presence of different concentrations of DOX (without ZnPc-PDT) and Cytotoxic effects of ZnPc-PDT (5 and 20 J/cm^2) with different concentrations of DOX (chemo-PDT); The results are expressed as mean ± SD (n = 3); *p < 0.02, **p < 0.0001 versus control; (D) Combination Index of chemo-PDT for determination of antagonism (CI > 1.0); additive effects (CI = 1.0) and synergism (CI < 1.0) were calculated according to Combination Index (CI) studies [26].

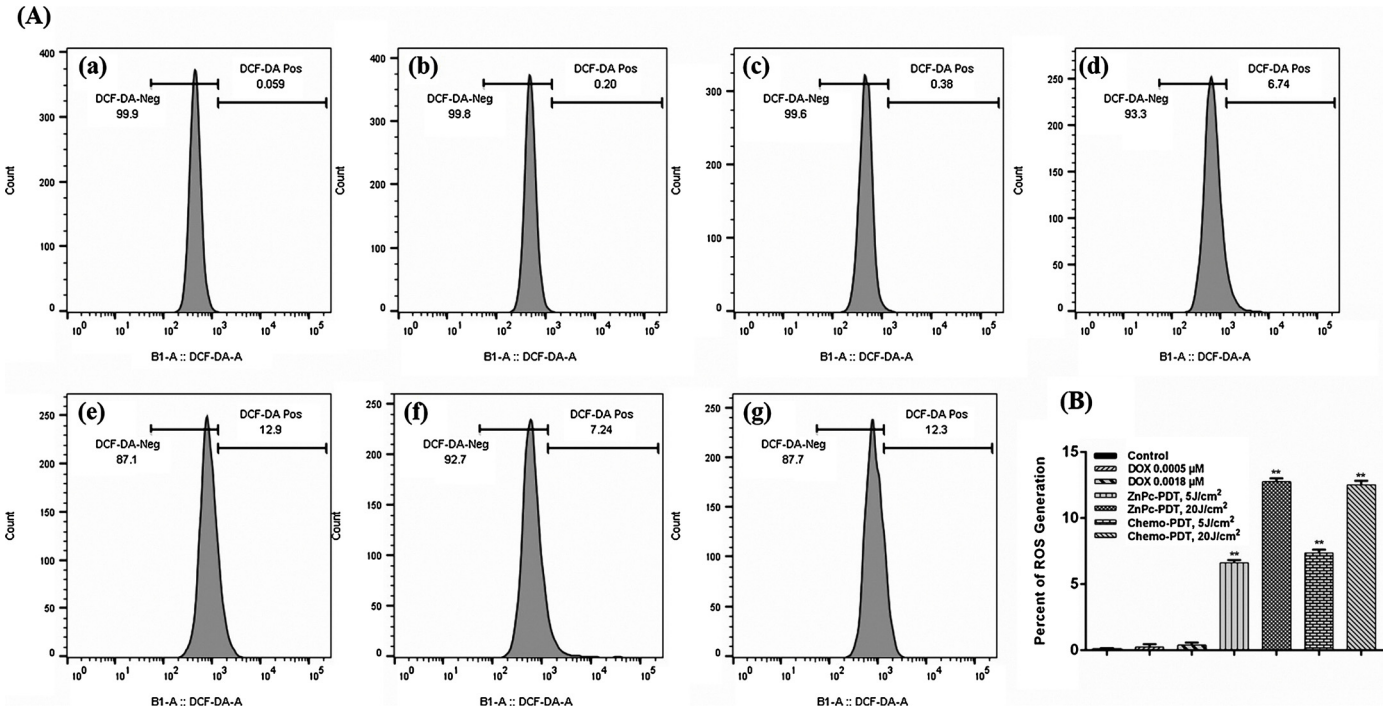

Fig. 3. ROS generation after treatment with DOX, ZnPc-PDT and chemo-PDT. (A) Flow cytometry histograms. Control (a); cells were treated with DOX (0.0005 (b) and 0.0018 (c) μM), ZnPc-PDT (5 (d) and 20 (e) J/cm^2) and chemo-PDT (5 J/cm^2 with 0.0005 μM of DOX (f) and 20 J/cm^2 with 0.0018 μM of DOX (g)). 24 h after treatment cells were stained with DCFH-DA and fluorescence intensity was measured by flow cytometry. (B) ROS generation represent as mean ± SD (n = 3); **P < 0.0001 compared with control group.

No IC50 and CI values could be appointed for the combination of DOX and IC50 s values of ZnPc-PDT due to high toxicity to the chemo-PDT with ZnPc and DOX. Therefore, the IC50 s values of ZnPc-PDT have not been assayed in the further combination analyze with ZnPc-PDT and DOX.

3.4. Production of ROS

The light source of PDT must exhibit appropriate spectral characteristics that were matched with the maximum absorption wavelength of the ZnPc applied in order to generate sufficient ROS toward producing cytotoxic effects [27]. So, the ZnPc-PDT can obviously induce production of ROS, but, the production of ROS in chemo-PDT need to be clarified. 24 h after treated of cells in dark, the production of ROS was determined by flow cytometry. The chemotherapy group with the DOX showed no production of ROS compared to the control group (Fig. 3). On the other hand, the generation of ROS after ZnPc-PDT groups was significant compared to the control group, in particular, high dose of the laser. Also, the Chemo-PDT groups showed no production of ROS compared to the ZnPc-PDT groups. In fact, the combination of ZnPc-PDT and DOX led to a significantly generation of ROS; but, there were insignificant changes between the ZnPc-PDT groups and the chemo-PDT groups. Therefore, synergistic effects were not observed in the generation of ROS after chemo-PDT.

3.5. Chemo-PDT with ZnPc and DOX activated autophagy

One of the cellular and molecular pathways can be induced by PDT and chemotherapy is autophagy [28,29]. Autophagy is a self-degradative mechanism and lysosomal action for the recycling of organelles and proteins in live cells. Autophagy is an essential biological process and required for maintaining homeostasis and it participates in many aspects of proliferation, development, differentiation, metabolism, and aging of cells. Also, it can be activated by various conditions including lack of nutrients substances and oxidative stress [30]. So, we investigated whether DOX and ZnPc-PDT induces autophagy in SK-MEL-3 cells. The results of the live cells imaging system and flow cytometry instrument (Fig. 4) showed that DOX and ZnPc-PDT alone had no/ negligible palpable effects on autophagy activity. As well as, we investigated the effects of chemo-PDT on autophagy activity in cells. The results showed that the autophagy was activated in chemo-PDT groups after 24 h. Interestingly, in the high dose of laser nearly higher rate of autophagy were observed; thus, in this dose of PDT, the autophagy was more significantly increased than low dose of laser. So, we can understand the intricacy role of laser doses effects on the intracellular responses. The term “double-edged sword” is mentioned in many scientific articles and describes the role of autophagy in cancer that is very complex and paradoxical. Due to the paradoxical role of autophagy in cancer progression, the researches for determinate the definite role of autophagy in cancer treatment is still in beginning steps [31]. Accordingly, our data indicate that autophagy induced by chemo-PDT in SK-MEL-3 cells be able to serves as a pro-survival process and/or pro-death mechanism.

3.6. Acidic organelles were significantly increased after chemo- PDT with ZnPc and DOX

In the process of autophagy flux, the acidic state of the lysosome is a critical factor for activation of lysosomal enzymes [32]. In fact, decreased lysosomal acidity levels damage numerous vital cellular and molecular processes including the final steps of autophagy where autophagosomes fuse with lysosomes [33,34]. If chemo-PDT activated autophagy flux, the lysosomal acidity must be significantly increased after the chemo-PDT stress was imposed. So, for improved evidence of activated autophagy in chemo-PDT groups, we used Lysotracker Red DND-99 to determine the pH of lysosome qualitatively.

Therefore, in the present study, the red fluorescent intensity changes of lysosome were monitored. Upon to the data (Fig. 4D) of LysoTracker Red DND-99 staining, it is obvious that the red fluorescent intensity of lysosome in DOX and ZnPc-PDT investigated groups, was no

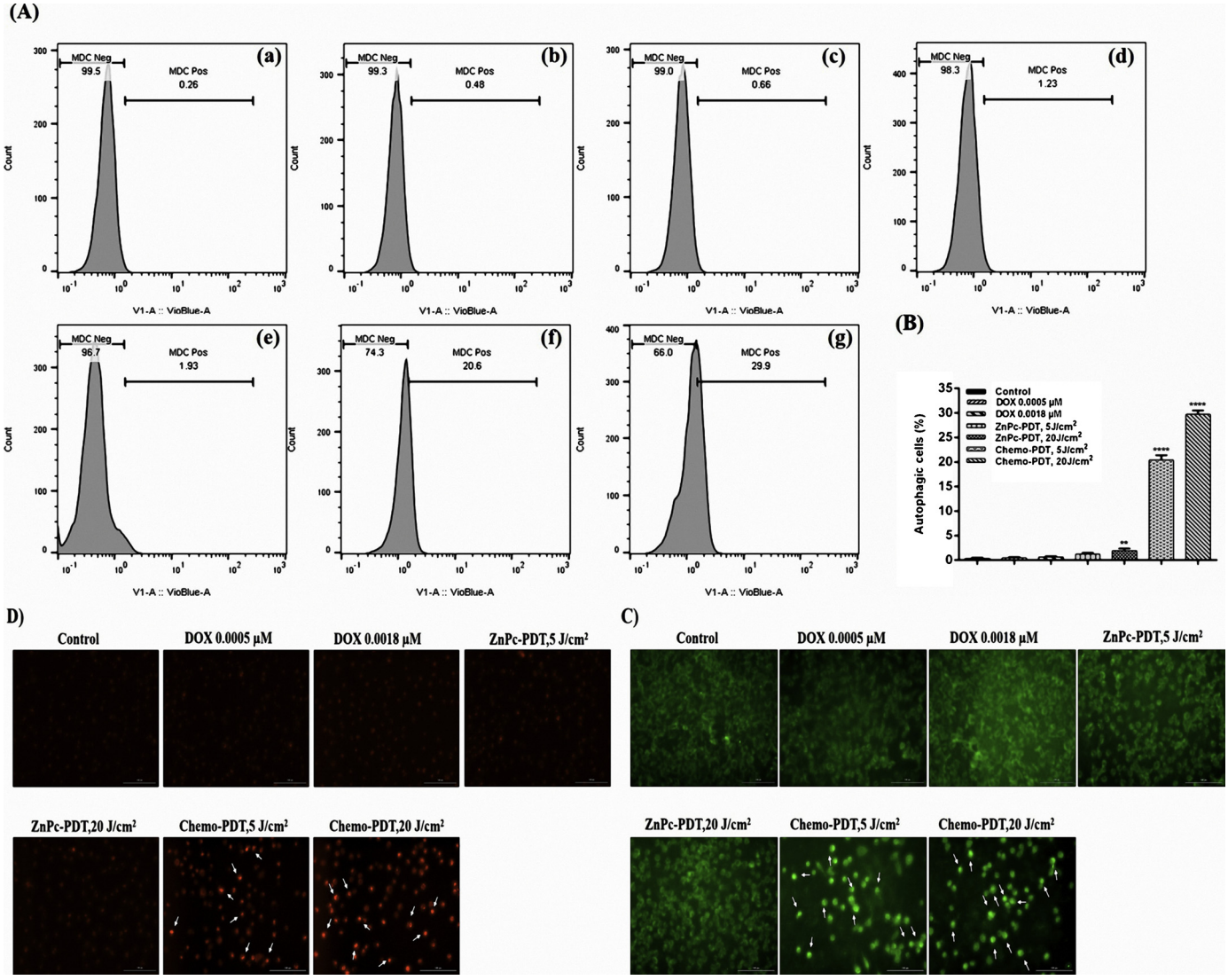

Fig. 4. Activation of autophagy after chemo-PDT. (A) Flow cytometry histograms. Control (a); cells were treated with DOX (0.0005(b) and 0.0018 (c) µM), ZnPc-PDT (5 (d) and 20 (e) J/cm^2) and chemo-PDT (5 J/cm^2 with 0.0005 µM of DOX (f) and 20 J/cm^2 with 0.0018 µM of DOX (g)). 24 h after treatment, cells were stained with MDC and fluorescence intensity was measured by flow cytometry. (B)The values are represented as mean ± SD (n = 3); **P < 0.001, ****P < 0.0001 compared with control group. (C) Representative images of autophagic cells (Green) detected by live cells imaging system. (D) Lysosomal acidic environment (Red) was detected after treatment with DOX, ZnPc-PDT and chemo-photodynamic by Lysotracker Red DND-99 staining live and cells imaging system on SK-MEL-3 cells.

significant changes in comparison to control group. Following by examining the changes of red fluorescent intensity of lysosome at chemo-PDT groups, it was found that autophagy in combination groups by an increase of lysosomal acidity. Finally, we can say that chemo-PDT with ZnPc and DOX can induce an autophagy flux in treated cells after 24 h, in particular high dose of the laser.

3.7. Chemo- PDT with ZnPc and DOX increased apoptosis on SK-MEL-3 cell line

Recent studies have reported that the generation of ROS may play a key role in sensitization to chemotherapy drugs in cancer cells [35]. Basically, the ROS generated by PDT is able to destroy cancer cells directly by necrosis and/or apoptosis cell death [36].

To evaluate the levels of apoptosis induced by chemo-PDT with ZnPc and DOX, we used ApoFlowEx® FITC Kit. As shown in Fig. 5, apoptotic cells in chemo-PDT groups were observed, which were significantly higher in the ZnPc-PDT and DOX groups. So, we can say that chemo-PDT can induce significantly high levels of apoptosis and remain the levels of necrosis insignificant.

To further confirm the apoptosis induced by ZnPc-PDT, DOX and chemo-PDT groups, DAPI staining was carried out. The results of DAPI staining confirmed again that chemo-PDT triggered high levels of cell apoptotic response compared with the ZnPc-PDT and DOX groups. Fig. 5C showed that the cells with nuclear fragmentation in DAPI staining were observed in all treatments. Compared with the ZnPc-PDT and DOX groups, fragmentation of nuclear was significantly increased in chemo-PDT groups. These results showed that ZnPc-PDT and DOX induced apoptosis and with the combination of ZnPc-PDT and DOX, the induction of apoptosis was increased obviously.

3.8. Caspase-8, -9, -3 and Bcl-2 genes expression

We investigated the molecular pathways responsible for the activation of apoptosis. Apoptosis can be initiated by two classic pathways, intrinsic and extrinsic. The most generally observed pathways of apoptosis involve the trigger of a cascade of caspases, basically caspases-8, -9, and -3, that cleave a series of proteins leading to the caspase-dependent apoptosis [17]. Nevertheless, appearing document from an increasing number of experimental results indicates a pathway

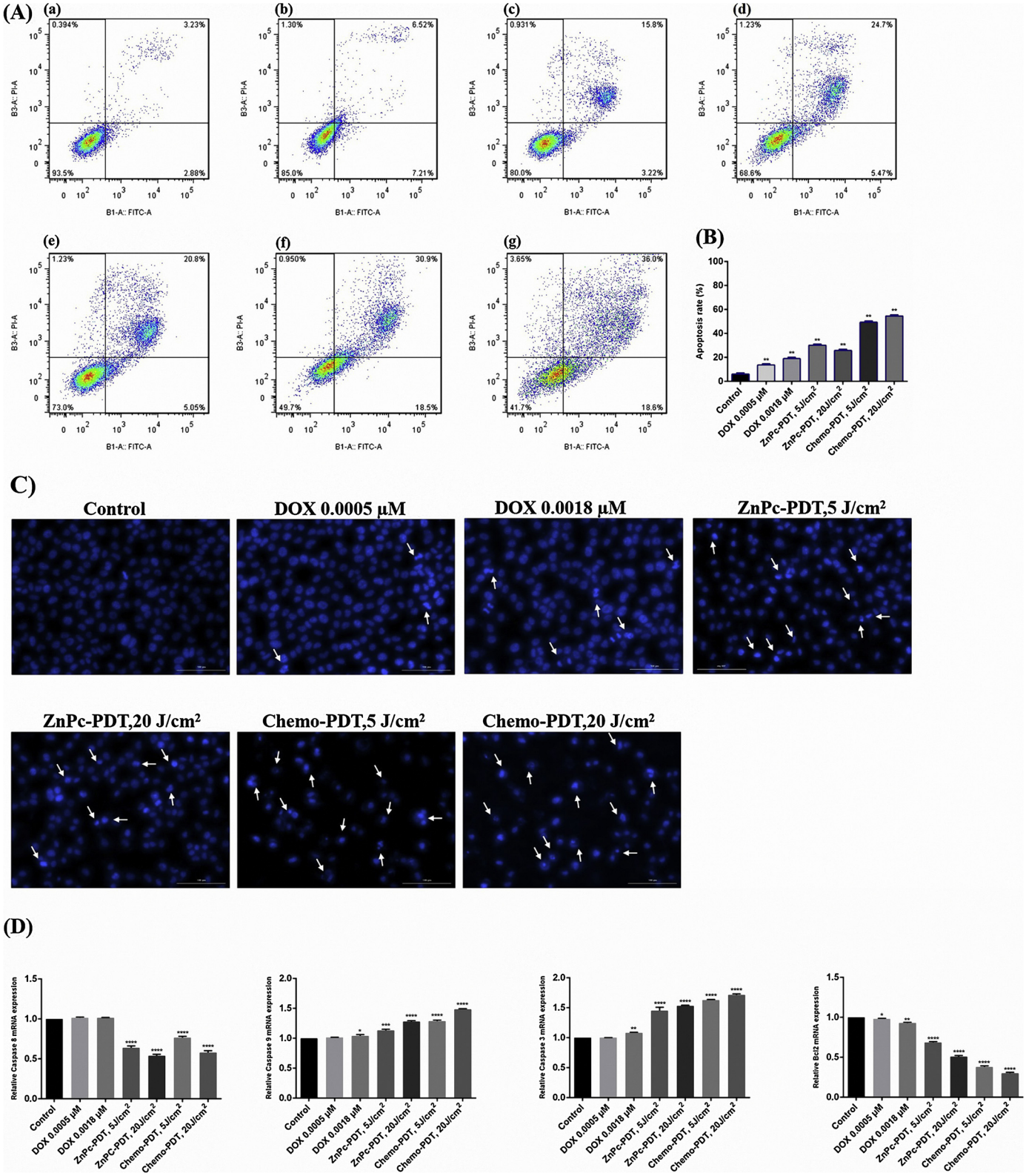

Fig. 5. DOX, ZnPc-PDT and chemo-PDT induced apoptosis (A) apoptosis and necrosis were determined at 24 h after treatments by flow cytometry. (a) control; cells were incubated with (DOX (0.0005 (b) and 0.0018 (c) μM), ZnPc-PDT (5 (d) and 20 (e) J/cm^2) and chemo-PDT (5 J/cm^2 with 0.0005 μM of DOX (f) and 20 J/cm^2 with 0.0018 μM of DOX (g)). (B) Data are means ± SD of three independent experiments and **$p < 0.0001$ versus control. (C) Staining of apoptotic nuclei by DAPI. (D) Caspase-8, Caspase-9, Caspase-3 and Bcl-2 genes expression in DOX, ZnPc-PDT and chemo-PDT were determined by qRT-PCR. Significant difference between Control and a treatment was indicated by *$p < 0.05$, **$p < 0.01$, ***$p = 0.0001$ and ****$p < 0.0001$ versus control.

in which apoptosis can active independently of caspases activation [37]. In this field, we have previously reported that in the lower dose of light source, the apoptosis pathway was probably caspase-independent [17]. In this study, apoptosis inducer molecular pathways after ZnPc-PDT, DOX and chemo-PDT were investigated on the SK-MEL-3 cells. As shown in Fig. 5D, following ZnPc-PDT, DOX and chemo-PDT treatment, we observed that the expression of caspase -9, -3 were significantly increased in SK-MEL-3 cells (except a lower dose of DOX). Also, we examined the gene expression changes of caspase -8. We observed that the gene expression of caspase -8 in all groups was significantly reduced in comparison to the control group (except a lower dose of DOX). The qRT-PCR results demonstrated that the caspase-dependent apoptosis pathway was evidently activated in all groups, except lower dose of DOX that the increase was not significant. Also, we examined the gene expression changes of Bcl-2 as an anti-apoptotic gene. As expected, we observed that the gene expression of Bcl-2 in all investigated groups was significantly reduced in comparison to the control group.

Therefore, we can conclude that the low dose of the light source maybe was not the only parameter involved in the activation of caspase-independent apoptosis in SK-MEL-3 cells. According to this, we can comprehend the very complex role of light source on the activation of caspase-dependent and caspase-independent apoptosis pathways and so more researches are needed in this field.

3.9. Cell cycle arrest after chemo- PDT with ZnPc and DOX

The cell cycle is the essential biological event having organized regulation in normal cells, which nearly generally become disturbed in cancer cells [38]. The arrest of the cell cycle is a critical event, and its consequences are very complex. Cell cycle arrest induced by anticancer treatments in some cases can result to activation apoptosis [39]. Thus, the potential effects of ZnPc-PDT, DOX and chemo-PDT on cell cycle arrest of SK-MEL-3 cells have been under focused.

In this regard, we examined the arrest of the cell cycle after treatment and cell cycle distribution was determined by flow cytometry. The results of cell cycle analysis allowed to allocate the cells to either subG1(fragmented DNA, apoptosis), G0/G1, S and G2/M phase population.

As shown in Fig. 6, flow cytometry results demonstrated that the control cells, primarily distributed of 0.99% in subG1, 93.70 in G0/G1, 2.55% in S and 2.91% in G2/M phase, were approximately viable and no cell death occurred. DOX groups were not showed significant differences to this distribution, except for a relatively small increase in the subG1 and G2/M phase of the cell cycle were found in the cells. While, after treatment with ZnPc-PDT, more cells were significantly appeared in subG1(18.20% in 5 J/cm^2 and 12.80% in 20 J/cm^2) and G2/M (11.70% in 5 J/cm^2 and 16.50% in 20 J/cm^2) phase. Interestingly, we found that highly subG1 (41.8% in 5 J/cm^2 and 33.6% in 20 J/cm^2) and G2/M (31.2% in 5 J/cm^2 and 40.4% in 20 J/cm^2) arrest was induced after chemo-PDT and it can stop the mitosis cell division strongly in SK-MEL-3 cells. Upon to the results of cell cycle distribution, we can observe the high effects of chemo-PDT on SK-MEL-3 cell cycle arrest.

3.10. Chemo- PDT with ZnPc and DOX decreased cell migratory ability

Cell migration is an acute factor in the process of tumor metastasis [40]. So, to further study the chemo-PDT potential, we evaluated its results on cell migration. In this regard, we found that cells of control and DOX groups almost totally covered the wound-scratch after 24 h (Fig. 7). It was indicative of high migratory ability of SK-MEL-3 cells. Also, we investigated whether ZnPc-PDT has inhibition effects on invasion and migration ability in SK-MEL-3 cells. After treated with ZnPc-PDT, the capacity of migration ability of the SK-MEL-3 cells was significantly decreased in the ZnPc-PDT groups compared with the control group. We further determined the cell migration ability after treatment with chemo-PDT. Outcomes of the wound-healing assay were certified that these chemo-PDT has higher ability to suppress SK-MEL-3 cell migration ability.

To create the results more convincing, we investigated genes expression levels of MMP-9 and Vimentin which may be related to SK-MEL-3 cell migration.

Our results showed (Fig. 7B), the gene expression of MMP-9 in ZnPc-PDT and chemo-PDT groups was significantly reduced in comparison to control group, which was significant at 5 J/cm^2 dose of laser in chemo-

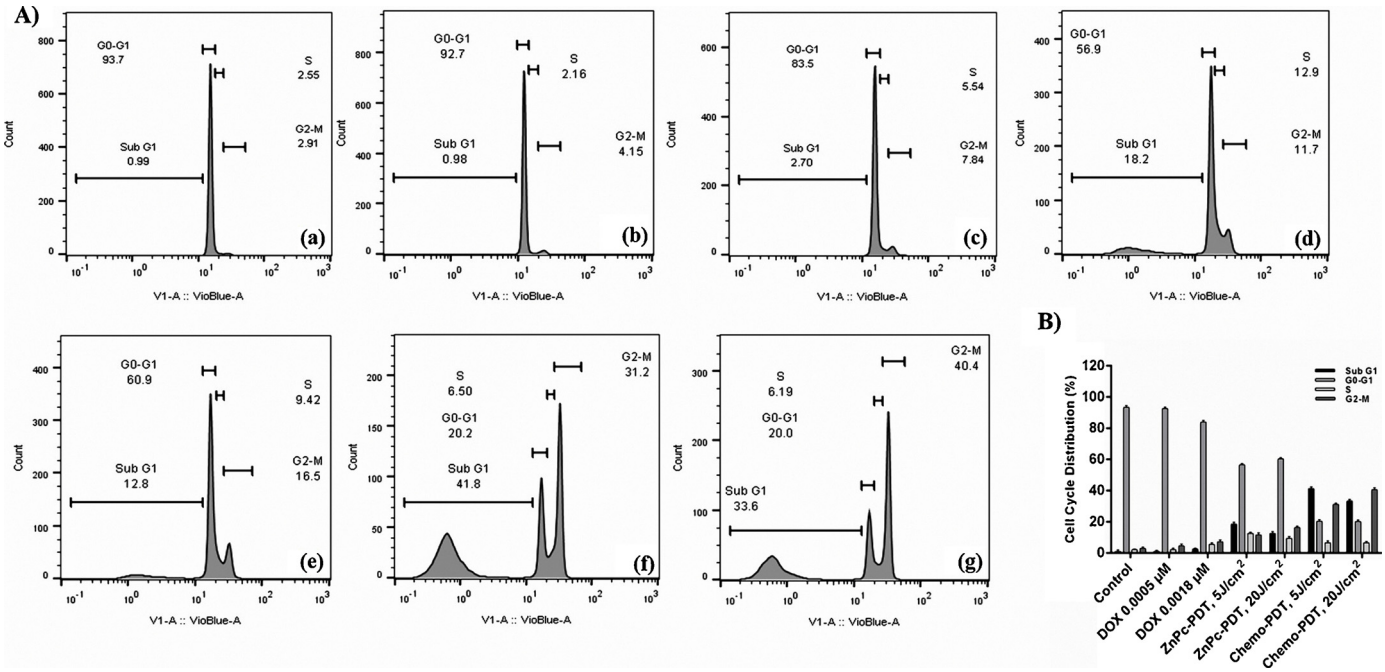

Fig. 6. Cell cycle distribution after treatment with DOX, ZnPc-PDT and chemo-PDT. (A) Cell cycle distribution was determined at 24 h after treatments by PI staining and flow cytometry. (a) Control; Cells were incubated with (DOX (0.0005 (b) and 0.0018 (c) μM), ZnPc-PDT (5 (d) and 20 (e) J/cm^2) and chemo-PDT (5 J/cm^2 with 0.0005 μM of DOX (f) and 20 J/cm^2 with 0.0018 μM of DOX (g)). (B)Data present three independent experiments versus control.

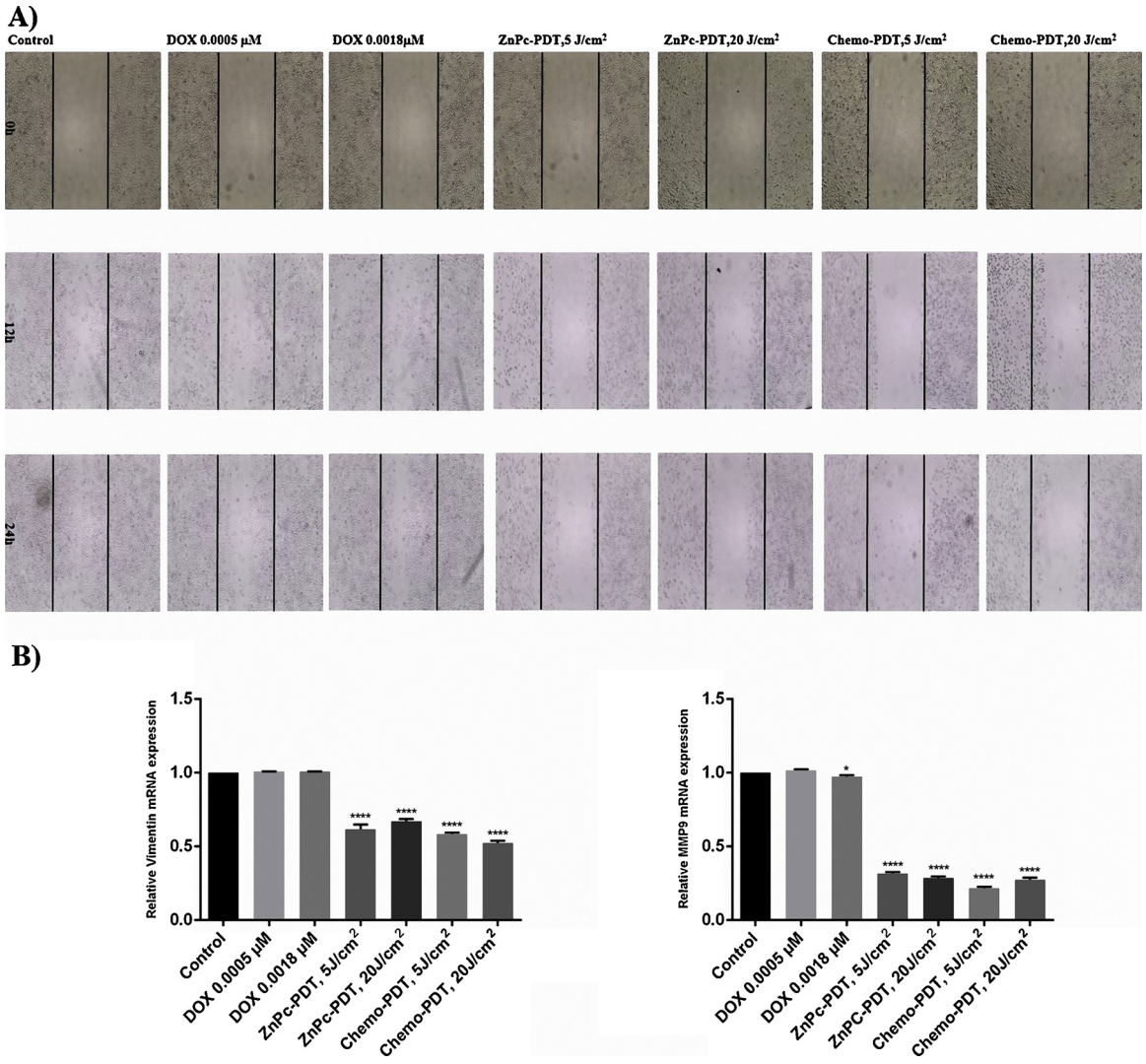

Fig. 7. The effects of DOX, ZnPc-PDT and chemo-PDT treatment cell migration. (A) After treatments, the cells were scratched and scratch areas were observed (0 h–24 h) and photographed by inverted microscope. (B) The effect of DOX, ZnPc-PDT and chemo-PDT treatment on Vimentin and MMP-9 on SK-MEL-3. Data are presented as means ± SD of three independent experiments and *p < 0.05, ****p < 0.0001 versus control.

PDT groups compared with the ZnPc-PDT. Also, the gene expression of Vimentin (Fig. 7B) in ZnPc-PDT and chemo-PDT groups was significantly reduced in comparison to control group, which was significant at 20 J/cm^2 dose of laser in chemo-PDT groups compared with the ZnPc-PDT.

Metastasis of melanoma is one of the leading causes of deaths from skin cancer and decrease rate of metastasis is the core of many research in the treatment of the melanoma. In this regard, these results certified that ZnPc-PDT and chemo-PDT have high ability to suppress melanoma cell migration.

4. Conclusion

Chemotherapy has always played and still play vital roles in melanoma treatment. Chemo-PDT is a powerful combination therapeutic approach with two anticancer strategies (PDT and chemotherapy) that can decrease the rate of metastasis and initiate melanoma cells death.

In 2016, studies by Tahmasebi et al. on melanoma cell line demonstrated that the melanoma cells incubated with 5-Aminolevulinic acid (5-ALA) and 5-fluorouracil(5-FU), enhanced the efficiency of 5-ALA-PDT [41].

In 2018, Gao et al. investigated the effect of polymeric micelles nanoplatforms on HepG2 human hepatocellular carcinoma cells (in vitro) and in mice (in vivo) for the co-delivery of DOX and ZnPc. All results showed increased cell death mainly through apoptosis and these polymeric micelles are promising nanoplatforms for the co-delivery of DOX and ZnPc for combination therapy [7]. Several studies have been published to co-delivery of DOX and ZnPc-PDT with different nanoparticles and methods. While, based on our study, pre-treatment with ZnPc-PDT has the high effects to more sensitize SK-MEL-3 cells to DOX, in particular low dose of diode laser.

In the present study, we found that pre-treatment with ZnPc-PDT at low dose of laser has shown the higher effects to sensitize melanoma cells toward the lower concentration of DOX. In another word, our studies proved low/insignificant effects of DOX in lower concentration, while in combinatorial ZnPc-PDT, chemo-PDT can inverse some mechanisms of resistance to DOX with triggering several anticancer biological processes including autophagy activation, cell cycle arrest, reduced cell migration ability and increase apoptosis.

Moreover, we found that pre-treatment with ZnPc-PDT at high dose of laser has shown approximately higher effects on activation of biological pathways such as autophagy in melanoma cells. So, the applied light sources have a predominant role in determining the CI and molecular pathways of chemo-PDT that can be useful for melanoma treatment with non-invasive and fewer side effects.

Many of strategies have been examined to enhance the efficacy of

chemotherapy drugs, such as; autophagy activators, cell cycle and cell migration inhibitors, apoptosis inducers agents and nanoparticles. Based on this study, PDT is a manageable and powerful anti-cancer treatment that may provide a replacement for most of these combinatorial factors. However, further investigations for the exact illumination of chemo-PDT mechanisms in different cancers are still needed.

Funding

Michael R Hamblin was supported by USNIH grant R01AI050875.

References

[1] American Cancer Society, Cancer Facts & Figures 2018, American Cancer Society, Atlanta, 2018.
[2] Z. Chen, et al., Zinc phthalocyanine conjugated with the amino-terminal fragment of urokinase for tumor-targeting photodynamic therapy, Acta Biomater. 10 (10) (2014) 4257–4268.
[3] H. Lee, et al., Combination of chemotherapy and photodynamic therapy for cancer treatment with sonoporation effects, J. Control. Release (2018).
[4] L.N. Abdullah, E.K.-H. Chow, Mechanisms of chemoresistance in cancer stem cells, Clin. Transl. Med. 2 (1) (2013) 3.
[5] M. Aris, M.M. Barrio, Combining immunotherapy with oncogene-targeted therapy: a new road for melanoma treatment, Front. Immunol. 6 (2015) 46.
[6] Y. Huang, W. Sadée, Membrane transporters and channels in chemoresistance and-sensitivity of tumor cells, Cancer Lett. 239 (2) (2006) 168–182.
[7] D. Gao, P.-C. Lo, Polymeric micelles encapsulating pH-responsive doxorubicin prodrug and glutathione-activated zinc (II) phthalocyanine for combined chemotherapy and photodynamic therapy, J. Control. Release (2018).
[8] U. Gatzemeier, et al., Randomized phase II trial of gemcitabine–cisplatin with or without trastuzumab in HER2-positive non-small-cell lung cancer, Ann. Oncol. 15 (1) (2004) 19–27.
[9] C.-M.J. Hu, L. Zhang, Nanoparticle-based combination therapy toward overcoming drug resistance in cancer, Biochem. Pharmacol. 83 (8) (2012) 1104–1111.
[10] M.C. Li, et al., Effects of combined drug therapy on metastatic cancer of the testis, Jama 174 (1291) (1960) p. 1960-1299.
[11] N.P. Brodin, C. Guha, W.A. Tomé, Photodynamic therapy and its role in combined modality anticancer treatment, Technol. Cancer Res. Treat. 14 (4) (2015) 355–368.
[12] A. Khdair, et al., Nanoparticle-mediated combination chemotherapy and photodynamic therapy overcomes tumor drug resistance in vitro, Eur. J. Pharm. Biopharm. 71 (2) (2009) 214–222.
[13] W. Park, et al., Advanced smart-photosensitizers for more effective cancer treatment, Biomater. Sci. 6 (1) (2018) 79–90.
[14] D. Luo, et al., Chemophototherapy: an emerging treatment option for solid tumors, Adv. Sci. 4 (1) (2017) 1600106.
[15] Q. Chen, et al., Photodynamic therapy guidelines for the management of oral leucoplakia, Int. J. Oral Sci. 11 (2) (2019) 14.
[16] M. Wainwright, H. Smalley, C. Flint, The use of photosensitisers in acne treatment, J. Photochem. Photobiol. B, Biol. 105 (1) (2011) 1.
[17] M.A. Doustvandi, et al., The interaction between the light source dose and caspase-dependent and-independent apoptosis in human SK-MEL-3 skin cancer cells following photodynamic therapy with zinc phthalocyanine: a comparative study, J. Photochem. Photobiol. B, Biol. 176 (2017) 62–68.
[18] E. Buytaert, M. Dewaele, P. Agostinis, Molecular effectors of multiple cell death pathways initiated by photodynamic therapy, Biochimica et Biophysica Acta (BBA)-Reviews on Cancer 1776 (1) (2007) 86–107.
[19] C. Vogel, C. Hager, H. Bastians, Mechanisms of mitotic cell death induced by chemotherapy-mediated G2 checkpoint abrogation, Cancer Res. 67 (1) (2007) 339–345.
[20] T. Yan, et al., pH-Sensitive mesoporous silica nanoparticles for chemo-photodynamic combination therapy, Colloids Surf. B Biointerfaces 161 (2018) 442–448.
[21] Z. Luksiene, Hypericin as novel and promising photodynamic therapy tool: studies on intracellular accumulation capacity and growth inhibition efficiency, Medicina Kaunas (Kaunas) 39 (7) (2003) 677–682.
[22] R. Ritz, et al., In vitro comparison of hypericin and 5-aminolevulinic acid-derived protoporphyrin IX for photodynamic inactivation of medulloblastoma cells, PLoS One 7 (12) (2012) e51974.
[23] H.-L. Xu, et al., Anti-proliferative effect of Juglone from Juglans mandshurica Maxim on human leukemia cell HL-60 by inducing apoptosis through the mitochondria-dependent pathway, Eur. J. Pharmacol. 645 (1–3) (2010) 14–22.
[24] J. Nackiewicz, M. Kliber-Jasik, M. Skonieczna, A novel pro-apoptotic role of zinc octacarboxyphthalocyanine in melanoma me45 cancer cell's photodynamic therapy (PDT), J. Photochem. Photobiol. B, Biol. 190 (2019) 146–153.
[25] W. Lü, et al., Synthesis and photoactivity of pH-responsive amphiphilic block polymer photosensitizer bonded zinc phthalocyanine, Sci. China Chem. 55 (6) (2012) 1108–1114.
[26] J.C. Ashton, Drug combination studies and their synergy quantification using the chou–Talalay method, Cancer Res. 75 (11) (2015) 2400.
[27] K. Plaetzer, et al., Photophysics and photochemistry of photodynamic therapy: fundamental aspects, Lasers Med. Sci. 24 (2) (2009) 259–268.
[28] E. Buytaert, et al., Deficiency in apoptotic effectors Bax and Bak reveals an autophagic cell death pathway initiated by photodamage to the endoplasmic reticulum, Autophagy 2 (3) (2006) 238–240.
[29] J.J. Reiners, et al., Assessing autophagy in the context of photodynamic therapy, Autophagy 6 (1) (2010) 7–18.
[30] S. Li, et al., Autophagy activation alleviates nonylphenol-induced apoptosis in cultured cortical neurons, Neurochem. Int. 122 (2019) 73–84.
[31] M. Russo, G.L. Russo, Autophagy inducers in cancer, Biochem. Pharmacol. 153 (2018) 51–61.
[32] C. Settembre, et al., Signals from the lysosome: a control centre for cellular clearance and energy metabolism, Nat. Rev. Mol. Cell Biol. 14 (5) (2013) 283.
[33] H.L. Best, et al., Characterisation of early changes in ovine CLN5 and CLN6 batten disease neural cultures for the rapid screening of therapeutics, Neurobiol. Dis. 100 (2017) 62–74.
[34] C. Zhang, et al., Inhibition of autophagic degradation process contributes to Claudin-2 expression increase and epithelial tight junction dysfunction in TNF-α treated cell monolayers, Int. J. Mol. Sci. 18 (1) (2017) 157.
[35] C. Lange, P. Bednarski, Evaluation for synergistic effects by combinations of photodynamic therapy (PDT) with temoporfin (mTHPC) and Pt (II) complexes carboplatin, cisplatin or oxaliplatin in a set of five human cancer cell lines, Int. J. Mol. Sci. 19 (10) (2018) 3183.
[36] C.A. Robertson, D.H. Evans, H. Abrahamse, Photodynamic therapy (PDT): a short review on cellular mechanisms and cancer research applications for PDT, J. Photochem. Photobiol. B, Biol. 96 (1) (2009) 1–8.
[37] N.B.R. Vittar, et al., Caspase-independent apoptosis, in human MCF-7c3 breast cancer cells, following photodynamic therapy, with a novel water-soluble phthalocyanine, Int. J. Biochem. Cell Biol. 42 (7) (2010) 1123–1131.
[38] G.I. Evan, K.H. Vousden, Proliferation, cell cycle and apoptosis in cancer, Nature 411 (6835) (2001) 342.
[39] M. Devès, F. Bourrat, Transcriptional mechanisms of developmental cell cycle arrest: problems and models, Seminars in Cell & Developmental Biology, Elsevier, 2012.
[40] S. Yang, et al., Hinokiflavone induces apoptosis in melanoma cells through the ROS-mitochondrial apoptotic pathway and impairs cell migration and invasion, Biomed. Pharmacother. 103 (2018) 101–110.
[41] H. Tahmasebi, et al., Enhancing the efficiency of 5-aminolevulinic acid-mediated photodynamic therapy using 5-fluorouracil on human melanoma cells, Photodiagnosis Photodyn. Ther. 13 (2016) 297–302.